SIGNIFICANCE OF CENTRIFUGAL MODEL TEST IN SOIL MECHANICS

SIGNIFICATION DE L'ESSAI EN MODELE CENTRIFUGE DANS LE MECANIQUE DES SOLS

ЗНАЧЕНИЕ ЦЕНТРОБЕЖНОГО МОДЕЛИРОВАНИЯ В МЕХАНИКЕ ГРУНТОВ

M. MIKASA, Professor, Department of Civil Engineering, Osaka City University
N. TAKADA, Assistant, Department of Civil Engineering, Osaka City University, Japan

SYNOPSIS The significance of the centrifugal model test in soil mechanics is discussed in general aspect, and data of bearing capacity of sandy ground are presented to show the validity of the similarity law that a model reduced in size to a scale of 1/n and centrifuged to the acceleration of ng has an utterly similar stress pattern, and consequently similar strain pattern as the prototype soil structure. The movements of sand particles and the shape of the load-settlement curves clearly show the effect of dilatancy. The similarity law for stress- and time-dependent behavior in consolidation of soft clay is also discussed by using Mikasa's consolidation theory (1963, 1965) and the data of the centrifuged model test of self-weight consolidation. The observed data well coincide with what the theory predicted. A few examples of slide failures in c-materials are also presented to show the mode of failure under big self-weight.

INTRODUCTION

Soil engineering problems such as stability of slopes, earth pressure, bearing capacity, settlement, etc. are usually solved by using theories based on a set of simplified assumptions, which are not always considered valid and sometimes lead us to erroneous conclusions. Therefore prior to the construction of an important structure, it is desirable to conduct a large scale field test in order to get reliable data. However the cost and time it requires and the difficulty in controlling the test condition reduce the value of the field test for research purposes.

The laboratory model test, on the contrary, is easy to operate, and has an advantage in that the test conditions can be controlled at will. However a small model has a fatal deficiency in that the stress intensity by its self-weight is much smaller than in the prototype. For instance, slope models in c-materials cannot be brought to failure, so far as the same materials as that of the prototype is used. Another example is the case of bearing capacity of sandy ground. The stress in the model being very small, not only the value of bearing capacity, but also the strain patterns in the soil mass may be utterly different from those in the prototype owing to the effect of dilatancy. The behavior of a small model, any way, is supposed to be different from that of the prototype owing to the small self-weight stresses.

To place a small model in a centrifugal force field is a good and practically the only countermeasure to overcome this difficulty of the model test. By this means the stress pattern in the small model can be made the same to that in the prototype, as illustrated in Fig.1, and the strain patterns in both soil masses are expected to be similar, if not identical.

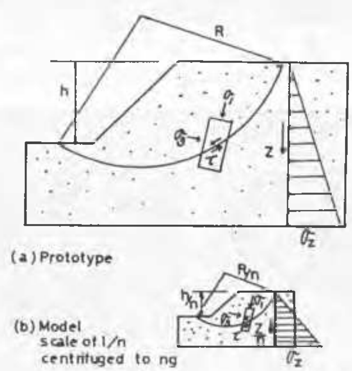

Fig. 1. Similarity between prototype and centrifuged model.

Realizing this point early, the authors developed and used a series of centrifugal testing apparatuses for the research works in soil mechanics problems---such as the self-weight consolidation of very soft clay, bearing capacity of sandy and clayey grounds, and stability of slopes and retaining walls(sheet pile) in clayey and sandy materials. We have since observed many interesting phenomena, and accumulated by this time substantial informations concerning the new testing method itself, and the behaviors of the soil structures under the actual stress conditions.

At the Mexico Conference we(Mikasa, Takada, and Yamada, 1969) reported the results of a series of centrifugal model tests for the stability of a rockfill dam. Another paper (Avgherinos and Schofield, 1969) based on the same principle was also presented at the Conference and results of stability tests on the slope model in saturated Kaoline were reported. Afterwards late Professor R.K, Roscoe referred to the importance of the centrifugal model testing in his Rankine Lecture(1971). We now wish to present here some of our data chiefly from the viewpoint of similarity and usefulness of the centrifugal model testing.

BEARING CAPACITY OF SANDY GROUND

We shall begin with a general consideration on the similarity of stress pattern taking the case of an elastic ground subjected to a uniform strip load. Dotted lines in Fig.2(a) show the contours of equal vertical stress both by the self-weight (γ = 1.6 t/m^3) and by the uniform load (B = 5 m, q = 10 t/m^2) applied on the ground surface. By superposing these we obtain the contours of composite vertical stress as shown in solid lines.

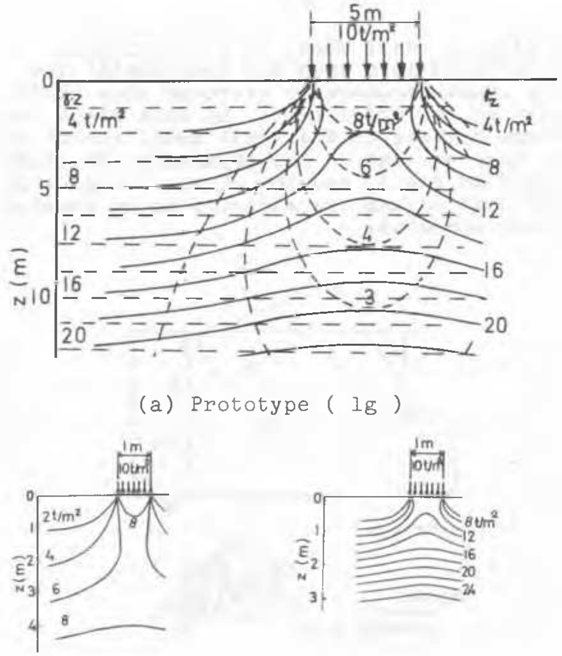

(a) Prototype (1g)

(b) Ordinary model (1g) (c) Centrifuged model (5g)

Fig. 2. Similarity of the vertical stress distribution in the ground under a strip load.

Fig.2(b) show the stress pattern when the width of the strip load is reduced to 1 m, which is utterly different from that shown in Fig.2(a), while if it is centrifuged to the acceleration of 5g, the stress pattern becomes similar to that of the prototype as shown in Fig.2(c). In this case not only the vertical stress σ_z but also every stress is identical to that in the prototype at geometrically similar point, and the strain pattern is also expected to be similar.

If the same soil, together with the same condition and the same stress,lead to the same behavior and the same strength, then a model reduced in size to a scale of 1/n and centrifuged to the acceleration of ng will have the same ultimate bearing capacity as the prototype. Terzaghi's equation

$$q_d = cN_c + \frac{1}{2}\gamma BN_\gamma + \gamma D_f N_q \qquad (1)$$

also leads to the same conclusion. As the values of c, N_c, N_γ, and N_q are the same in both cases, $1/n \cdot B$, $1/n \cdot D_f$ and $n\gamma$ will give the same value of q_d as that of the prototype.

Now we show some results of centrifugal loading tests for a sandy ground. Fig.3 shows the specimen box and the loading device in the centrifugal apparatus. They are attached to the rotating arm, and hang in the direction of the resultant of gravity force and centrifugal force. The loading jack is powered by an electric motor mounted on the rotating center shaft. The loading rate is regulated at 1 mm/min. The sand is a clean angular one, whose particle size ranges 0.074 - 2 mm, and was compacted to a relative density of 77% and saturated.

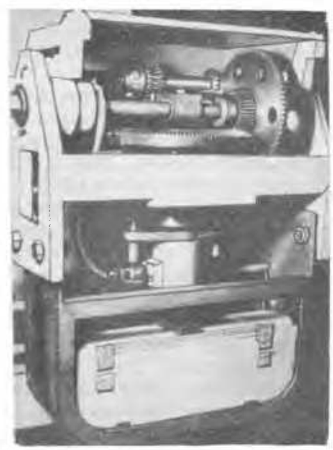

Fig. 3. Specimen box and loading device attached to the centrifuge.

Figs 4 and 5 are the load-settlement curves from two test series. In Fig.4 the footing width is kept constant and the acceleration is changed, while in Fig.5 the acceleration is kept constant and the footing width is changed. The same symbols in the curves indicate the equivalent prototype footing width B_p ($= n \cdot B_m$). The corresponding curves show the similar tendency, and the shapes of the curves change from general failure to local failure with the increase in the footing width or the acceleration by the effect of dilatancy.

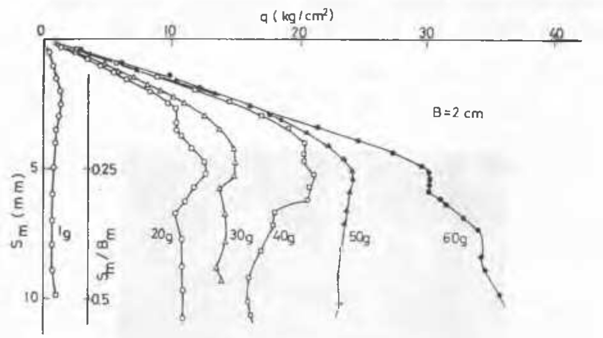

Fig. 4. Load-settlement curves for different accelerations.

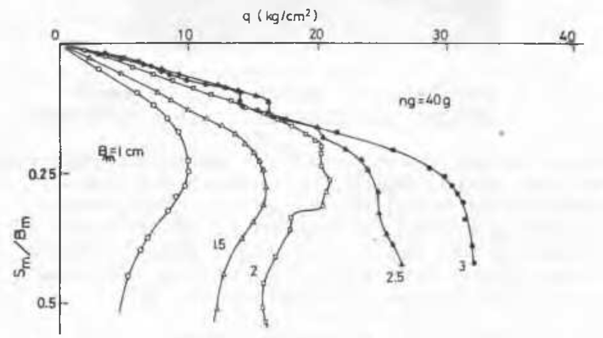

Fig. 5. Load-settlement curves for different footing widths.

The values of bearing capacity q_d, that are decided as the peak value of q for the case of general failure and as the yield value for the case of local failure, were plotted against B_m for different values of ng (Fig.6). It is seen that q_d varies proportionally both to B_m and n.

Reviewing Figs 4, 5 and 6, the similarity between the centrifuged model and the prototype may be said valid, though some minor factors have affected the shape of the load-settlement curves to some extent.

Figs 7 and 8 show the movements of the sand particles under loading. These were photographed by using a stroboscope and keeping the camera shutter open during the test. The

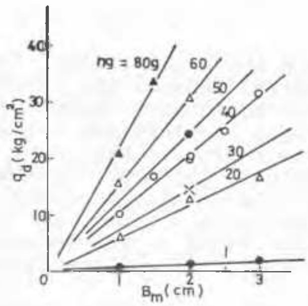

Fig. 6. Bearing capacity/footing width relationships for different accelerations.

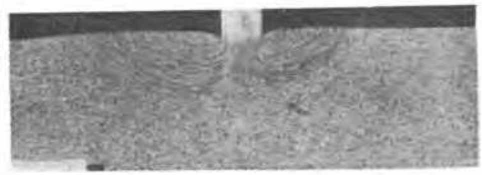

(a) Gravitational field (1g).

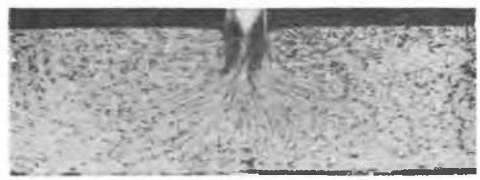

(b) Centrifugal acceleration field (40g)

Fig. 7. Particle movement in shallow foundation (B_m=2cm, D_f=0).

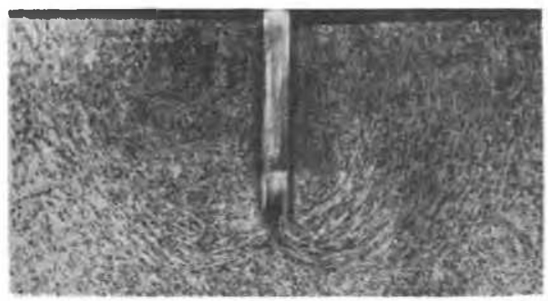

(a) Gravitational field (1g).

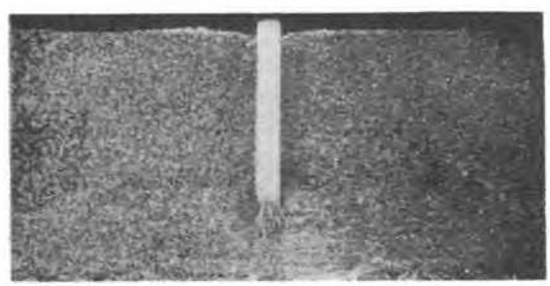

b) Centrifugal acceleration field (40g).

Fig. 8. Particle movement in deep foundation (B_m=1cm, D_f=6cm).

models tested in the gravitational field show the mode of general failure and clear slip surface is observed in both cases. Whereas in the centrifugal acceleration field of 40g, the slip surface cannot be seen, and the particles move radially outwards from the bottom of the footing. Especially in the case of D_f = 6 cm the particle movement is restricted to a narrow range owing to the volumetric reduction by the negative dilatancy under high stress.

SELF-WEIGHT CONSOLIDATION

Terzaghi's consolidation theory brought forth the similarity law that the time necessary for consolidation varies proportionally to the square of the thickness of clay layer. Mikasa (1963, 1965) investigated the consolidation of soft clay, in which the Terzaghi's assumption that m_v and k are constant is not valid, and found that the self-weight consolidation of very soft clay does not follow the above similarity law. The theory will be shown here briefly.

The differential equation for one-dimensional consolidation of homogeneous saturated clay, taking into consideration the effect of self-weight, is as follows:

$$\frac{\partial \zeta}{\partial t} = \zeta^2 \left\{ c_v \frac{\partial^2 \zeta}{\partial z_0^2} + \frac{dc_v}{d\zeta}\left(\frac{\partial \zeta}{\partial z_0}\right)^2 - \frac{d}{d\zeta}(c_v m_v \gamma') \frac{\partial \zeta}{\partial z_0} \right\} \quad (2)$$

where ζ is consolidation ratio (= f_0/f, where f = 1 + e is nominated as volume ratio), t is time, γ' is unit weight considering buoyancy, and z_0 is original coordinate (the coordinate z in the original state in which the clay is assumed to have a fairly big uniform volume ratio f_0 throughout the whole depth).

Changing Eq.(1) into dimensionless form using

$$T_v = c_{v0} t / \left(\frac{H_0}{2}\right)^2 \quad (3)$$

$$Z_0 = z_0 / H_0 \quad (4)$$

where c_{v0} : c_v in the original state.
H_0 : H in the original state.
we get

$$\frac{\partial \zeta}{\partial T_v} = \frac{\zeta^2}{4} \left\{ \phi(\zeta) \frac{\partial^2 \zeta}{\partial Z_0^2} + \frac{d\phi(\zeta)}{d\zeta}\left(\frac{\partial \zeta}{\partial Z_0}\right)^2 - \frac{d}{d\zeta}(\phi(\zeta) m_v \gamma) H_0 \frac{\partial \zeta}{\partial Z_0} \right\} \quad (5)$$

where $\phi(\zeta) = c_v / c_{v0}$

If the last term in parenthesis is negligibly small the aforementioned similarity is valid because the degree of consolidation becomes a function of T_v. However when the clay is very soft or its thickness is very large, the value of the term becomes too large to be neglected, and the same similarity does not hold.

Now by examining Eq.(5), however, we find that a model clay layer on centrifuge, having thickness H_0/n and increased unit weight $n\gamma'$ (considering buoyancy), will have the similar consolidation process to the prototype having thickness H_0 and unit weight γ', time scale being reduced as

$$\frac{t_m}{t_p} = \frac{H_m^2}{H_p^2} = \frac{1}{n^2} \quad (6)$$

where the suffixes m, p indicate the model and the prototype, respectively. And the scale ratio of settlement is given by

$$\frac{S_m}{S_p} = \frac{H_m}{H_p} = \frac{1}{n} \quad (7)$$

Fig. 9. Centrifugal model test of self-weight consolidation (in operation).

Fig.9 shows the centrifugal apparatus for self-weight consolidation in operation (photographed by using stroboscope). Two transparent specimen containers of 10 cm inner diameter are set in the steel vessels which hang freely from both ends of the rotating arm. The radius of rotation is 1m.

Fig.10 shows the time-settlement curves of a series of self-weight consolidation test for a remolded marine clay (LL=98.0%, PL=39.6%) in slurry state, the initial water content being kept w_0=200%. In this series the specimen thickness H_m and centrifugal acceleration ng were chosen in such a way that

$$n \times H_m = H_p = 5 \text{ m}$$

and the boundary conditions of both single drainage (base being impermeable) and double drainage were adopted. Fig.10 clearly shows the validity of the similarity laws (6) and (7).

Fig.11 shows the relationships between H_m and t_{50} for several test series. In test series shown in (a), including the data from Fig.10, the value n x H_m is kept constant so that the assumed prototype is identical, whereas in (b) the acceleration is kept constant and H_m is varied. Obviously the results are different.

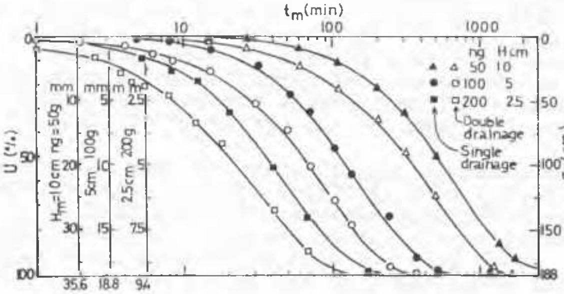

Fig. 10. Time-settlement curves for equivalent prototype thickness of H_p=5m, and w_o=200%.

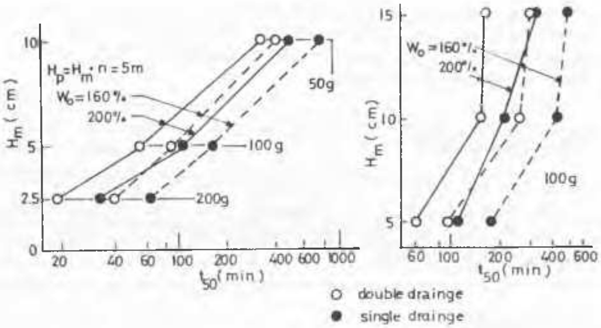

(a) Constant H_p of 5m. (b) Constant acceleration of 100g.

Fig. 11. Relation-ships between H_m and t_{50}.

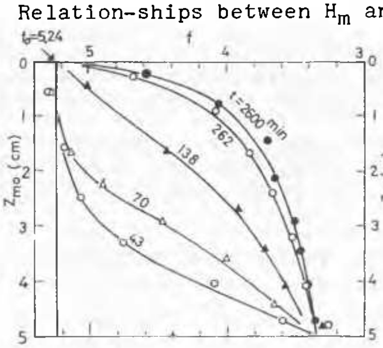

(a) Double drainage.

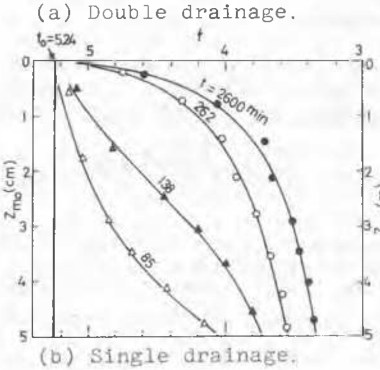

(b) Single drainage.

Fig. 12. Isochrones for the two boundary conditions (100g, H=5cm, w_o=160%).

The similarity law does not hold in series (b) and is valid in series (a), just as the theory predicted.

Fig.12 (a) and (b) show the distribution of volume ratio f(=1+e) plotted against original coordinate z_o at several stages in the consolidation process. Each isochrone was obtained by stopping the test at each stage and measuring the water content distribution by sampling a series of specimens along the depth. The shapes of the isochrones in the self-weight consolidation are quite different from those in the ordinary consolidation owing to the centrifugal or the gravity force downwards. These are very similar to those calculated by Mikasa's consolidation theory, and f - p relations of a very soft clay is easily obtained from the isochrone after the consolidation.

STABILITY TESTS FOR c-MATERIALS

Here we wish to present a few examples of stability tests on slopes and cantilever sheet pilings in c-materials. The testing apparatus used here is the same to that described in our previous paper (Mikasa, Takada and Yamada, 1969). Figs 13, 14 and 15 are the illustrations of failures, and Table 1 shows the test conditions and the results. The models are put in the centrifugal acceleration field, the strength of which being increased gradually till the failure takes place. The critical height of the slope or the sheet pilings of the corresponding prototype is calculated by

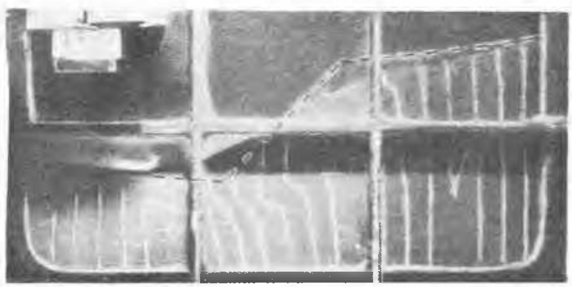

Fig. 13. Failure of a slope (field block sample; under test).

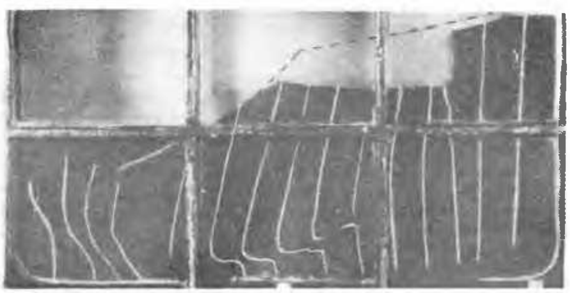

Fig. 14. Failure of a slope (consolidated block sample; after test).

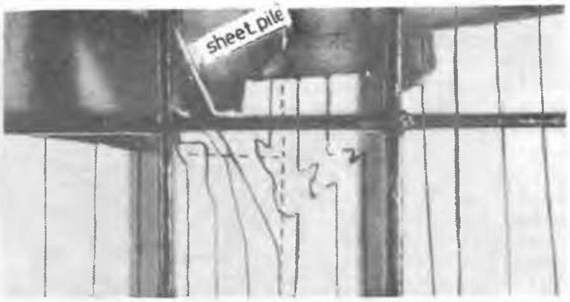

Fig. 15. Failure of a cantilever sheet piling (after test).

the equation

$$h_{pcr} = n_{cr} \cdot h_m \quad (8)$$

where n_{cr} is a critical acceleration ratio at which the failure occurred.

As to the mode of failure for slopes shown in Figs 13 and 14, a circular slip surface is seen, and for the sheet piling in Fig.15 discrete triangle wedges are seen. It is noteworthy that in both cases the active part in the slide surface seems to form a shear plane, whereas the passive part clearly forms a shear zone. This tendency was observed in almost every case, and suggests the mechanism of failure subjected to the actual big self-weight.

As to the similarity law shown in Eq.(8), there is no reason to doubt from the theoretical point of view. However the effects of some secondary factors such as the properties concerning the consolidation or the rheology, together with the effect of the boundary of the specimen container, make it difficult to analyse the test data strictly enough to check the similarity law. For this reason no such data are presented in this paper.

CONCLUSIONS

1) Bearing capacity of saturated sandy ground was tested by centrifuged model . The results show the validity of the similarity law that the model reduced to a scale of 1/n and centrifuged to the acceleration of ng has a similar stress and strain pattern as the prototype. The movements of sand particles and the shape of load-settlement curves change under different self-weight by the effect of dilatancy.

2) Self-weight consolidation of very soft clay was tested by centrifuged models. The results showed good agreement with the conclusions of Mikasa's consolidation theory. The similarity law $t \propto H^2$ does not hold for the ordinary self-weight consolidation, and is valid for the centrifuged model that has the same acceleration ratio n (=α/g) to the factor by which the model scale is reduced.

3) A few examples of failures of slopes and sheet piling in c-materials are presented which show a characteristic mode of failure under big self-weight.

ACKNOWLEDGEMENTS

The authors wish to express their thanks to Mr. A. Isono, Mr. K. Yamada, Mr. M. Fujii and Mr. A. Mochizuki for assistance with their experimental works.

REFERANCES

AVGHERINOS, P.J. and SCHOFIELD, A.N. (1969) Drawdown failures of centrifugal models, Proc. 7th Int. Conf. Soil Mech., II, pp. 497-505.

MIKASA, M. (1963), The consolidation of soft clay --- A new consolidation theory and its application, Kazima Kenkyusyo Syuppankai, Tokyo.(in Japanese;synopsis(1965) in English)

MIKASA, M., TAKADA, N. and YAMADA, K. (1969) Centrifugal model test of a rockfill dam, Proc. 7th Int. Conf. Soil Mech., II, pp. 325-333.

ROSCOE, K.H. (1970), The influence of strains in soil mechanics, 10th Rankine Lecture, Geotechnique vol.20, No.2, p.167.

Table 1, Stability Tests on Centrifuged Models.

soil structure	Material	Acceleration at failure	Critical slope height	Illustration
Slope Hm=8cm 1:1	Field undisturbed block sample; consolidated by self-weight at an acceleration of 100g before trimmed into a slope. w_L=55.8, wp=28.3, q_u=0.8kg/cm² (after consolidation)	130g	h_{pcr}=10.4 m h_{cr} calculated from q_u is 13.6m	Fig.13
Slope Hm=8cm 1:1	Block sample; consolidated from a slurry under a pressure of 1kg/cm². w_L=89.2, wp=37.8, q_u=0.6kg/cm²	130g	h_{pcr}=10.4 m h_{cr} calculated from q_u is 10.1m	Fig.14
Cantilever sheet piling Hm=8cm vertical	Kaolin-plaster mixture aged for 24 hours; extremely sensitive. q_u=0.64kg/cm² Model sheet pile; 0.8mm thick steel plate, lower end fixed.	125g	h_{pcr}=10.0 m Model sheet pile is equivalent to 100mm thick steel plate	Fig.15